Designing light-emitting diode arrays for uniform near-field irradiance

Ivan Moreno, Maximino Avendaño-Alejo, and Rumen I. Tzonchev

We analyze the first-order design of light sources consisting of multiple light-emitting diodes (LEDs) to uniformly illuminate a near target plane by considering each single LED as an imperfect Lambertian emitter. Simple approximate equations and formulas are derived for the optimum LED-to-LED spacing, i.e., the optimum packaging density, of several array configurations to achieve uniform near-field irradiance. © 2006 Optical Society of America

OCIS codes: 150.2950, 230.3670.

1. Introduction

The rapid development of light-emitting diodes (LEDs) over the past few years has surpassed the characteristics of incandescent lamps in luminous efficiency, durability, reliability, safety, and power requirements.[1,2] Though modern high-power LEDs produce up to 120 lm per device, several individual LEDs must be mounted on panels to obtain practical powers. Nevertheless, in many lighting applications a uniform illumination distribution is desired, which is affected by both the packing density and the array configuration of LEDs.[3] The illumination nonhomogeneity is appreciable when the panel–target distance is not much longer than the panel size, for instance, LED systems that produce directional lighting, such as display lighting,[4,5] machine vision,[6,7] and microscopy.[8]

In this paper we analyze the optimum packaging density of LED arrays, i.e., the optimum LED-to-LED spacing, to achieve uniform near-field irradiance. We examine the characteristics of illumination uniformity for several array configurations considering each LED as an imperfect Lambertian emitter. Design expressions are derived for the optimum LED-to-LED distance for basic configurations of LED arrays. We analyze LED panels in the absence of any diffuser component[9,10] to create practical design tools for a wider variety of illumination systems.

2. Preliminaries

A. Assumptions

The precise illumination uniformity requirements depend on the particular application. The perceived illumination homogeneity depends on several factors, including distance of the observer from the target field, incidence angle of illuminating beam, background luminance, target reflectance, target pattern, and target color. To create a practical design tool for uniform illumination, we analyze only the irradiance distribution over a flat area parallel to the surface of the LED array. For some applications, the illuminated surface may be the diffusing sheet of a luminary.

Optically, we consider that each single LED produces a nonperfect Lambertian distribution of light. This approximation is valid for most LEDs without encapsulant (including stripe and tapered superluminescent LEDs)[11] and for spherically encapsulated LEDs in which the chip size is small with respect to the lens radius (e.g., large-encapsulant LEDs with multiple chips and single-chip LEDs). Also, because the emitting region of LEDs is typically less than 1 mm on a side, its irradiance variation with distance will be approximated with the inverse square law for a point source. The derived formulas and equations are then valid for panel–target distances $> 10A_{\mathrm{LED}}^{1/2}$ (A_{LED} is the LED emitting area), e.g., for typical panel–target distances >1 cm. Additionally, we will

I. Moreno (imoreno@planck.reduaz.mx) and R. I. Tzonchev are with Facultad de Fisica, Universidad Autonoma de Zacatecas, Apartado Postal C-580, 98060 Zacatecas, Zacatecas, Mexico. M. Avendaño-Alejo is with Centro de Ciencias Aplicadas y Desarrollo Tecnologico, Universidad Nacional Autónoma de México, Apartado Postal 70-186, 04510 Mexico Distrito Federal, Mexico.

Received 19 April 2005; revised 24 July 2005; accepted 27 July 2005.

0003-6935/06/102265-08$15.00/0

© 2006 Optical Society of America

assume that all the LEDs of each array will have equal values of radiant flux, and equal distributions in space and wavelength.

B. Optical Model from a Single LED

Ideally, a LED source is a Lambertian emitter, which means the irradiance distribution is also a cosine function of the viewing angle. In practice, this dependence turns out to be a power law that primarily depends on the encapsulant and semiconductor region shapes. A practical approximation for the irradiance distribution is given by[12]

$$E(r,\ \theta) = E_0(r)\cos^m \theta, \tag{1}$$

where θ is the viewing angle and $E_0(r)$ is the irradiance (W/m^2) on axis at distance r from the LED. The value of m depends on the relative position of the LED emitting region from the curvature center of the spherical encapsulant. If the chip position coincides with the curvature center, the number $m \approx 1$, and the source is nearly a perfect Lambertian (e.g., some Lumileds and Lamina LEDs). Typical LEDs often have values of $m > 30$, and the drop of intensity with the viewing angle is pronounced. The number m is given by the angle $\theta_{1/2}$ (a value typically provided by the manufacturer, defined as the view angle when irradiance is half of the value at 0°):

$$m = \frac{-\ln 2}{\ln(\cos \theta_{1/2})}. \tag{2}$$

The irradiance distribution given by Eq. (1) for a LED displaced to position (x_0, y_0) over a panel plane can be written in terms of Cartesian coordinates (x, y, z). The irradiance over every point (x, y) on a flat screen at distance z from the LED array may then be expressed as

$$E(x,\ y,\ z) = \frac{z^m L_{\mathrm{LED}}\, A_{\mathrm{LED}}}{\left[(x-x_0)^2 + (y-y_0)^2 + z^2\right]^{(m+2)/2}}, \tag{3}$$

where L_{LED} is the radiance ($W\ m^{-2}\ sr^{-1}$) of the LED chip and A_{LED} is the LED emitting area (m^2).

In practice, the nonhomogeneity and shape irregularities of low-quality encapsulating materials also affect the irradiance distribution of LEDs. However, the main source of irregularities in the irradiance distribution of LEDs is the small mirror placed behind the chip to increase the flux. Modern high-brightness phosphor LEDs have high-quality encapsulants and the phosphor layer avoids the imperfections due to the back mirror. As a result, the irradiance pattern is nearly that which is produced by Eq. (1). To create a practical design tool for a quick estimation, we will not consider these problems. We will use the irradiance distribution given by Eq. (3) for each single LED, and all LEDs of each array will have equal values of m and $L_{\mathrm{LED}}\, A_{\mathrm{LED}}$. An exception appears in Subsection 3.C and the last part of Subsection 3.D, where we use a different relative flux for the central LED.

3. Design Equations and Formulas for Uniform Irradiance

We now proceed to derive the design equations and formulas to obtain a uniform irradiance distribution for several geometries of LED arrays. In Subsection 3.A, we consider the simplest case, a two-LED array.

A. Two-LED Array

In this case, the irradiance E is given by the sum of the irradiances for two LEDs (the space between these LEDs is d):

$$E(x,\ y,\ z) = z^m A_{\mathrm{LED}} L_{\mathrm{LED}} \left\{ \left[\left(x - \frac{d}{2}\right)^2 + y^2 + z^2 \right]^{-(m+2)/2} + \left[\left(x + \frac{d}{2}\right)^2 + y^2 + z^2 \right]^{-(m+2)/2} \right\}. \tag{4}$$

The distance d can be adjusted so that the irradiance distribution is uniform over a larger region compared to the small uniform region illuminated by each single LED. The idea is to separate the two irradiance patterns so as to eliminate the minimum between the maxima from the two patterns. This idea is similar to Sparrow's criterion used in image resolution, which is given by a maximally flat condition.[13] Therefore, we can adjust the separation of the LEDs so that the implicit second-order term (inverse square law) of Eq. (4) vanishes, i.e., the irradiance slope variation is minimized. Differentiating E twice and setting $\partial^2 E/\partial x^2 = 0$ at $x = 0$ and $y = 0$ eventually yields the maximally flat condition for d:

$$d_0 = \sqrt{\frac{4}{m+3}}\, z, \tag{5}$$

where z is the distance from the center of the array to the target center. Figure 1(a) shows the illuminated screen by a two-LED array. Figure 1(b) shows the irradiance distribution along the x direction for a selected value of $m = 80.7$ (for a typical $\theta_{1/2} = 7.5°$), $z = 1$, and $d = d_0 = 0.219$. As shown in Fig. 1(b), the irradiance distribution is constant over the flat region in front of the LED array on the screen. Figure 1(c) shows the corresponding pattern when the separation between LEDs is slightly increased ($d = 1.18 d_0$).

B. Circular Ring LED Array

In machine vision applications, the most popular LED source is the ring array. We consider the case of a circular ring array of LEDs with radius ρ. Here the irradiance E is given by the sum of the irradiances for $N \geq 3$ LEDs:

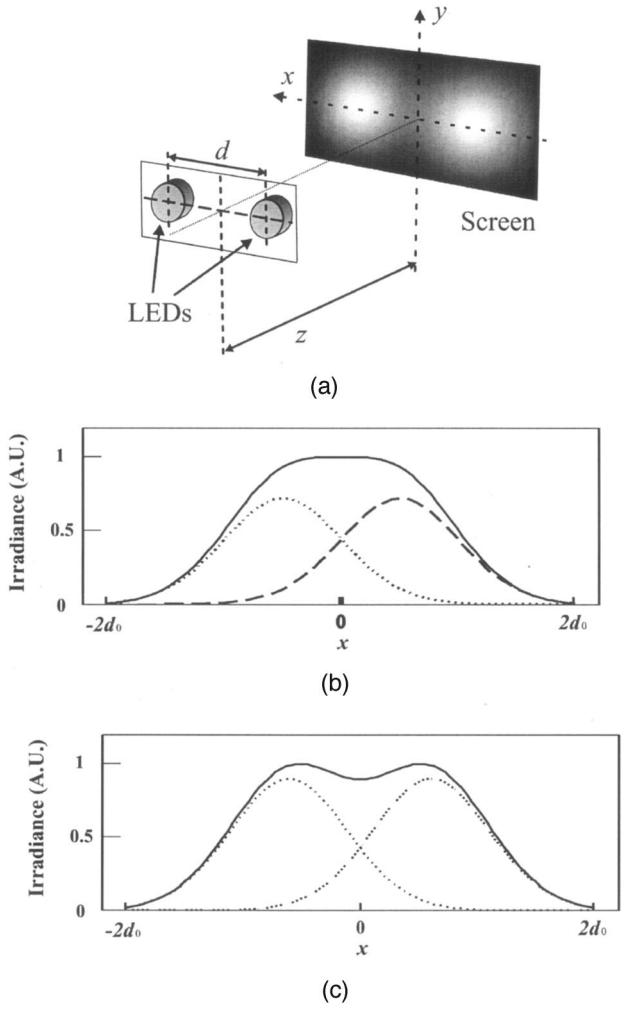

Fig. 1. Two-LED array. (a) Schematic illustration of the LED array with a screen at a distance z. (b) The uniform irradiance distribution (normalized to its maximum value) along the x direction at $y = 0$ for $m = 80.7$ and $d = d_0 = 0.219$. The dotted curves show the irradiance patterns of each single LED. (c) Corresponding pattern when the separation between LEDs is slightly increased.

$$E(x, y, z) = z^m A_{\mathrm{LED}} L_{\mathrm{LED}} \sum_{n=1}^{N} \left\{ \left[x - \rho \cos\left(\frac{2\pi n}{N}\right) \right]^2 + \left[y - \rho \sin\left(\frac{2\pi n}{N}\right) \right]^2 + z^2 \right\}^{-(m+2)/2}. \quad (6)$$

The ring radius ρ can be adjusted so that irradiance is almost uniform over a central region on the screen, and particularly uniform along the lines with directions $\langle \cos(2\pi n/N),\ \sin(2\pi n/N) \rangle$. As in the two-LED array, we can adjust the radius of the ring so that the implicit second-order term of Eq. (6) vanishes. The symmetry makes the problem one dimensional so that without loss of generality we can calculate the maximally flat condition along any radial axis that crosses a LED, such as the x axis at $y = 0$. The ring radius is then optimized to eliminate the central minimum of the resulting pattern. Differentiating E twice and setting $\partial^2 E/\partial x^2 = 0$ at $x = 0$ and $y = 0$ eventually yields the maximally flat condition

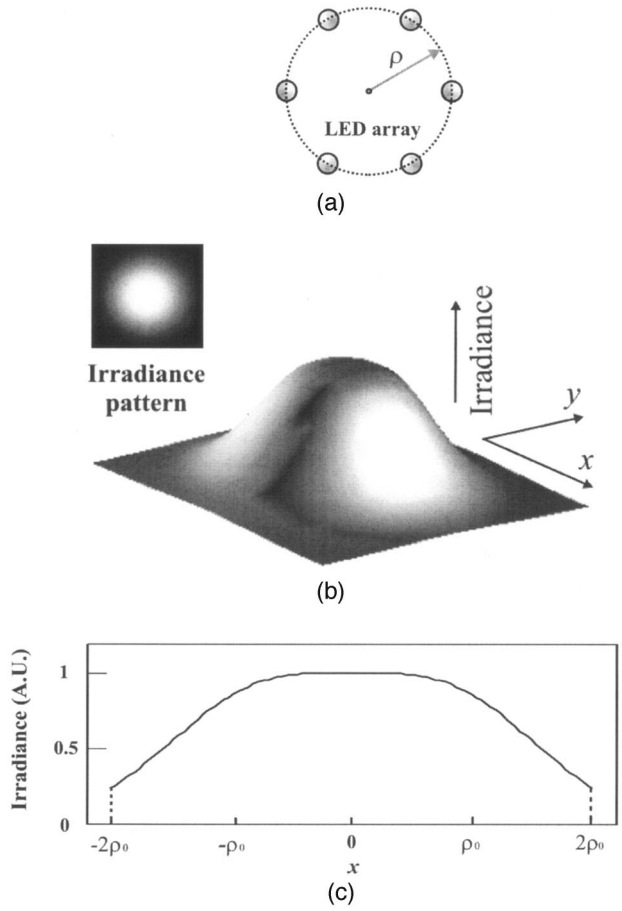

Fig. 2. Circular ring LED array. (a) Schematic illustration of an array with $N = 6$. (b) The uniform irradiance distribution of this array when $m = 30$ and $\rho = \rho_0 = 0.25$. (c) Corresponding normalized irradiance graph along the x direction at $y = 0$.

$$\rho_0 = \sqrt{\frac{2}{m+2}}\, z. \quad (7)$$

It is interesting to note that this design condition is independent of the number N of LEDs that assemble the ring. Figure 2(a) shows a circular ring array of six LEDs. Figure 2(b) shows the uniform irradiance pattern of this array for selected values of $m = 30$, $z = 1$, and $\rho = \rho_0 = 0.25$. Figure 2(c) shows the resulting irradiance pattern along the x direction at $y = 0$.

For ring arrays with three LEDs, the analytic condition given by Eq. (7) yields a flat irradiance pattern over a small central region around the triangle centroid. Numerical computations give an empirical condition to obtain a larger flat region:

$$\rho_0 = \sqrt{\frac{1.851}{m+2.259}}\, z. \quad (8)$$

C. Circular Ring LED Array with One LED in the Center

In medical lighting, a popular array in LED lanterns is a circular ring with one LED in the center, e.g.,

LED lamps used by dentists in curing processes.[14] Here we consider a circular ring array of N LEDs with one LED in the center. To obtain a flat pattern with this type of array, the relative power of the middle LED must be adjusted. The irradiance E is then given by the sum of the irradiances for $(N + 1) \geq 4$ LEDs:

$$E(x, y, z) = z^m A_{\mathrm{LED}} L_{\mathrm{LED}} \left(\sum_{n=1}^{N} \left\{ \left[x - \rho \cos\left(\frac{2\pi n}{N} \right) \right]^2 + \left[y - \rho \sin\left(\frac{2\pi n}{N} \right) \right]^2 + z^2 \right\}^{-(m+2)/2} + \phi \{ x^2 + y^2 + z^2 \}^{-(m+2)/2} \right), \quad (9)$$

where ϕ is the relative flux ($\phi = \Phi_{\mathrm{center}}/\Phi_{\mathrm{ring}}$) of the middle LED ($\Phi_{\mathrm{center}}$) with respect to the power (Φ_{ring}) of one LED over the ring.

Differentiating Eq. (9) twice and setting $\partial^2 E/\partial x^2 = 0$ at $x = 0$ and $y = 0$ eventually gives the condition for uniform irradiance

$$\rho_0 = \sqrt{\frac{4}{m+2}}\, z. \quad (10)$$

This condition is again independent of the number N of LEDs that assemble the ring: however, the optimum relative flux ϕ_0 linearly depends on N:

$$\phi_0 = N \left(\frac{m+2}{m+6} \right)^{(m+6)/2}. \quad (11)$$

Figure 3(a) shows a classic array, a ring of six LEDs with one middle LED. Figure 3(b) shows the irradiance pattern of this array for selected values of $m = 30$, $z = 1$, $\rho = \rho_0 = 0.354$, and $\phi_0 = 0.72$. Figure 3(c) shows the resulting irradiance pattern along the x direction at $y = 0$.

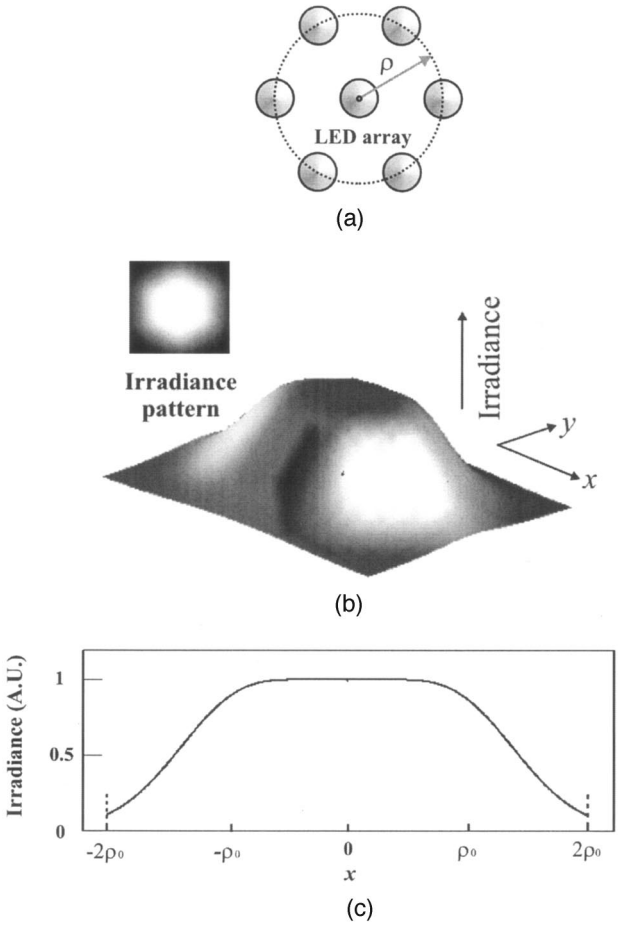

Fig. 3. Circular ring LED array with one LED in the center. (a) Schematic illustration of an array with $(N + 1) = 7$. (b) The uniform irradiance distribution of this array when $m = 30$, $\rho = \rho_0 = 0.354$, and $\phi_0 = 0.72$. (c) Corresponding normalized irradiance graph along the x direction at $y = 0$.

D. Linear LED Array

In structured lighting, the most popular LED source is the linear array of LEDs. We consider a linear array with a LED-to-LED separation d. In this case, irradiance E is given by the sum of the irradiances for N LEDs:

$$E(x, y, z) = z^m A_{\mathrm{LED}} L_{\mathrm{LED}} \sum_{n=1}^{N} \{ [x - (N + 1 - 2n)(d/2)]^2 + y^2 + z^2 \}^{-(m+2)/2}. \quad (12)$$

The maximally flat condition obtained by differentiating E twice and setting $\partial^2 E/\partial x^2 = 0$ at $x = 0$ and $y = 0$ eventually gives the expression

$$f(D) = \sum_{n=1}^{N} \left[(N + 1 - 2n)^2 (D^2/4) + 1 \right]^{-(m+6)/2} \times \left[1 - (m+3)(N + 1 - 2n)^2 (D^2/4) \right], \quad (13)$$

which yields the maximally flat condition for d (where $D = d/z$) as a function of m and N. When N is an even number, the maximally flat condition, $D = d_0/z$, is given by the zero cross of the f function. If $N = 2$, the resulting condition gives Eq. (5). In the case of N odd, the maximally flat condition is given by the minimum of Eq. (13). An analytical solution for these general cases proved difficult. However, when numerical values for m and N are provided, the solution can be easily obtained with any mathematical program.

Figure 4 illustrates the irradiance pattern for a linear array of seven LEDs with a selected value of $m = 80.7$ (for $\theta_{1/2} = 7.5°$). Figure 4(b) shows the uniform irradiance distribution of this array when $z = 1$ and $d = d_0 = 0.135$. Figure 4(c) shows the corresponding irradiance graph along the x direction at $y = 0$.

For arrays larger than four LEDs ($N > 4$ and $m > 30$), one empirical formula is

$$d_0 = \sqrt{\frac{3.2773}{m + 4.2539}}\, z. \quad (14)$$

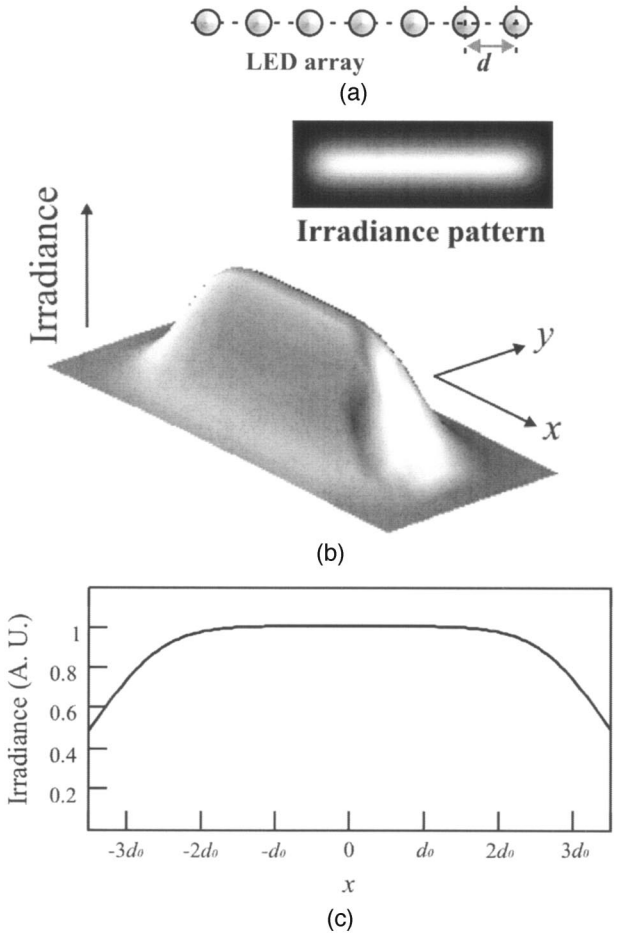

Fig. 4. Linear array of LEDs. (a) Schematic illustration of an array with $N = 7$. (b) The uniform irradiance distribution of this array when $m = 80.7$ and $d = d_0 = 0.135$. (c) Resulting normalized irradiance graph along the x direction at $y = 0$.

Equation (14) does not give a perfect flat irradiance like Eq. (13), but does guarantee that the ideal irradiance uniformity ($E_{\min}/E_{\max}$) over the central region of the pattern is more than 98%.

For an array with three LEDs, the maximally flat condition given by Eq. (13) gives a homogeneous pattern but not a flat irradiance pattern. To obtain a flat pattern, the relative flux of the middle LED must be adjusted. Differentiating E twice and setting $\partial^2 E/\partial x^2 = 0$ at $x = 0$ and $y = 0$ then gives the maximally flat condition:

$$d_0 = \sqrt{\frac{12}{m+3}}\, z. \tag{15}$$

The optimum relative flux $\phi_0 = \Phi_{\text{center}}/\Phi_{\text{lateral}}$ (where Φ_{center} is the LED power of the middle LED, and the other LEDs have a Φ_{lateral} power) is

$$\phi_0 = 4\left(\frac{m+3}{m+6}\right)^{(m+6)/2}. \tag{16}$$

Figure 5 illustrates the uniform irradiance pattern

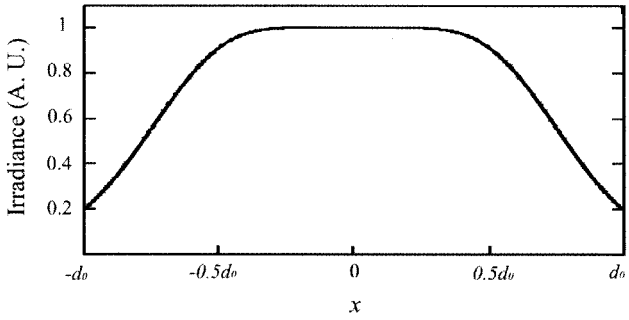

Fig. 5. Uniform irradiance pattern (along the x direction at $y = 0$) for a linear array of three LEDs with $m = 30$, $d = d_0 = 0.603$, and $\phi_0 = 0.835$.

(along the x direction at $y = 0$) for a linear array of three LEDs with $m = 30$, $z = 1$, $d = d_0 = 0.603$, and $\phi_0 = 0.835$.

E. Square LED Array

In terms of assembly requirements, the most popular extended LED array is the square, for example, in surgical lighting.[15] For a square array of LEDs the irradiance E is given by the sum of the irradiances of a matrix of $N \times M$ LEDs:

$$E(x, y, z) = z^m A_{\text{LED}} L_{\text{LED}} \times \sum_{i=1}^{N}\sum_{j=1}^{M} \{[x - (N+1-2i)(d/2)]^2 + [y - (M+1-2j)(d/2)]^2 + z^2\}^{-(m+2)/2}. \tag{17}$$

Differentiating Eq. (17) twice and setting $\partial^2 E/\partial x^2 = 0$ at $x = 0$ and $y = 0$ gives the expression

$$f(D) = \sum_{i=1}^{N}\sum_{j=1}^{M} (\{[(N+1-2i)^2 + (M+1-2j)^2](D^2/4) + 1\}^{-(m+6)/2}\{1 - [(m+3)(N+1-2i)^2 - (M+1-2j)^2](D^2/4)\}), \tag{18}$$

which yields the maximally flat condition for d (where $D = d/z$) as a function of m, N, and M. When both N and M are even numbers, the maximally flat condition, $D = d_0/z$, is given by the zero cross of the f function. If both N and M are odd, the maximally flat condition is provided by the minimum of Eq. (18). For all other possibilities, the maximally flat condition is given by the zero cross or by the first minimum of $f(D)$.

Figure 6 illustrates the irradiance pattern for a square array of 49 LEDs with $N = 7$, $M = 7$, and $m = 50$. Figure 6(b) shows the uniform irradiance distribution of this array when $z = 1$ and $d = d_0 = 0.17$. Figure 6(c) shows the corresponding irradiance graph along the x direction at $y = 0$.

The particular condition for a 2×2 array can be obtained from Eq. (7), for a circular ring array with $N = 4$, which leads to

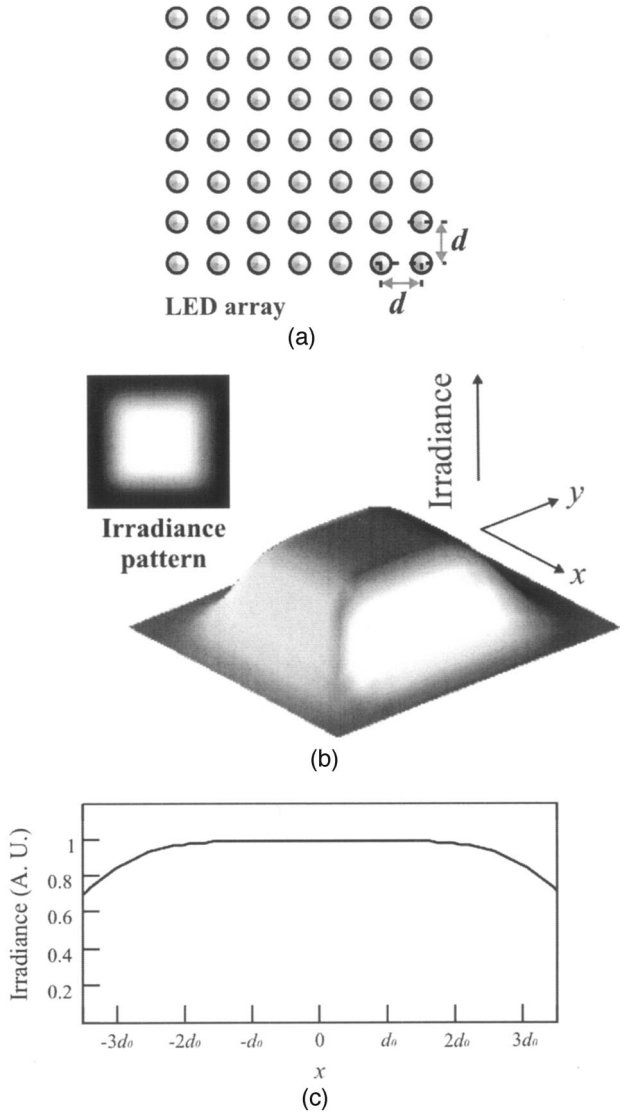

Fig. 6. Square array of LEDs. (a) Schematic illustration of an array with $N = 7$ and $M = 7$. (b) The uniform irradiance pattern when $m = 50$ and $d = d_0 = 0.17$. (c) Corresponding normalized irradiance distribution along the x direction at $y = 0$.

$$d_0 = \sqrt{\frac{4}{m+2}}\, z. \tag{19}$$

For arrays larger than 4×4 LEDs ($N \times M > 4 \times 4$ and $m > 30$), an empirical formula is

$$d_0 = \sqrt{\frac{1.2125}{m-3.349}}\, z. \tag{20}$$

Equation (20) does not give a perfect flat pattern as does Eq. (18) but it does ensure that the irradiance uniformity over the central region of the pattern is more than 97%.

F. Triangular LED Array

The triangular array, also called hexagonal, is a popular LED source owing to its packaging capabilities. For a triangular array, irradiance E is given by the sum of the irradiances for an array of $\{(N \times M) - 0.25[2M + (-1)^M - 1]\}$ LEDs:

$$E(x, y, z) = z^m A_{\mathrm{LED}} L_{\mathrm{LED}} \sum_{j=1}^{M} \sum_{i=1}^{N_-} \{[x - (N_+ - 2i)(d/2)]^2 + [y - (M + 1 - 2j)(\sqrt{3}d/4)]^2 + z^2\}^{-(m+2)/2}, \tag{21}$$

where $N_\pm = N + [(-1)^j \pm 1]/2$. The maximally flat condition obtained by differentiating E twice and setting $\partial^2 E/\partial x^2 = 0$ at $x = 0$ and $y = 0$ eventually gives the expression

$$f(D) = \sum_{j=1}^{M} \sum_{i=1}^{N_-} (\{[(N_+ - 2i)^2 + 3/4(M + 1 - 2j)^2](D^2/4) + 1\}^{-(m+6)/2} \{1 - [(m+3)(N_+ - 2i)^2 - 3/4(M + 1 - 2j)^2](D^2/4)\}), \tag{22}$$

which yields the maximally flat condition for d (where $D = d/z$) as a function of m, N, and M. When both N and M are even numbers, the maximally flat condition, $D = d_0/z$, is given by the zero cross of the f function. If both N and M are odd, the maximally flat condition is provided by the minimum of Eq. (22). For all other situations, the maximally flat condition is given by the zero cross or by the first minimum of $f(D)$.

Figure 7 illustrates the irradiance pattern for a triangular array of 46 LEDs with $N = 7$, $M = 7$, and $m = 50$. Figure 7(b) shows the uniform irradiance distribution of this array when $z = 1$ and $d = d_0 = 0.192$. Figure 7(b) shows the corresponding irradiance graph along the x direction at $y = 0$.

Comparing Figs. 7(c) and 6(c) seemingly indicates that the triangular array concentrates more energy within the flat area. Moreover, because the area of the triangular array is larger than that of the square, $A_{\mathrm{triangular}}/A_{\mathrm{square}} = 1.105$, we apparently may homogeneously illuminate a larger area (using an array with fewer LEDs) with a triangular array than with a square array. This can be better appreciated graphing the enclosed fraction of the radiated energy against increments in an area (centered) of the illuminated screen (see Fig. 8). We chose a square as the shape of the enclosing area for the square array, and for the triangular array, we chose a rectangle (with proportions equal to the array). Although the power fraction depends on the size of the illuminated area in the same way for the square array as for the triangular array, Fig. 8 indicates that the enclosed power that falls within the area in front of the array is larger in the triangular array (0.716) than in the square array (0.673). Therefore, working at optimum packaging density the triangular array can project a larger fraction of the emitted power inside the uniform core region than the square array.

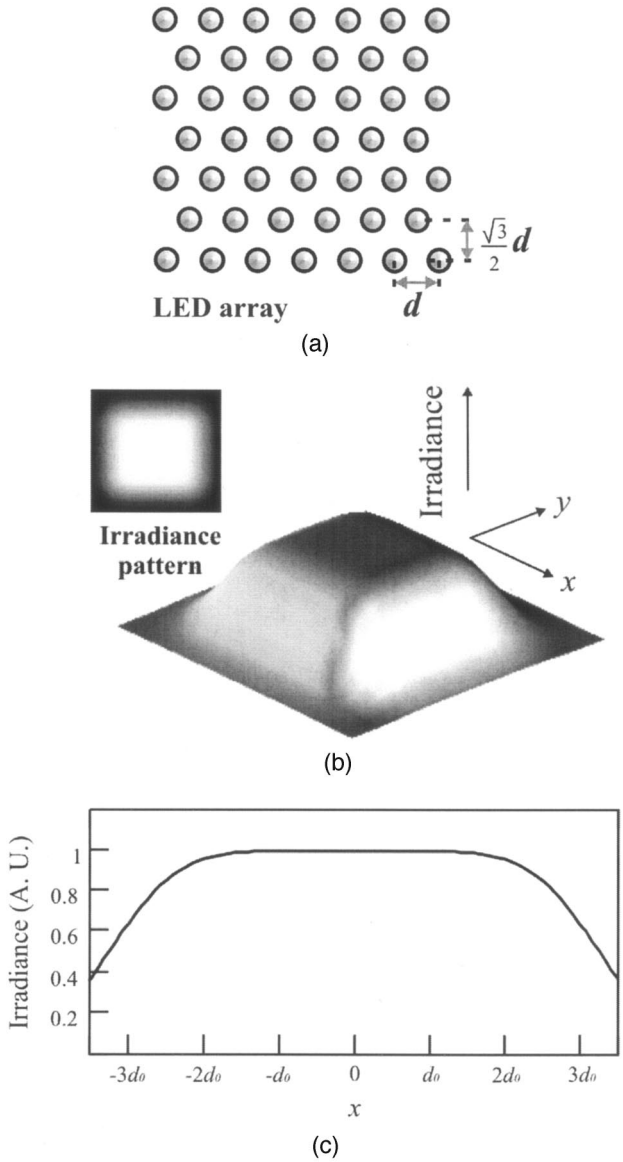

Fig. 7. Triangular array of LEDs. (a) Schematic illustration of an array with 46 LEDs ($N = 7$ and $M = 7$). (b) The uniform irradiance pattern when $m = 50$ and $d = d_0 = 0.192$. (c) Corresponding normalized irradiance distribution along the x direction at $y = 0$.

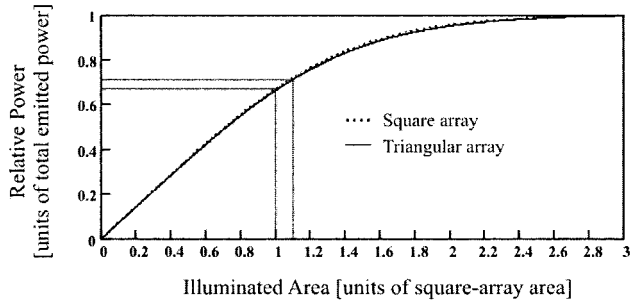

Fig. 8. Relative power distribution plot. The curve indicates the fraction of power of the total flux in an illuminated pattern that falls within a square (for the square array) or a rectangle (for the triangular array).

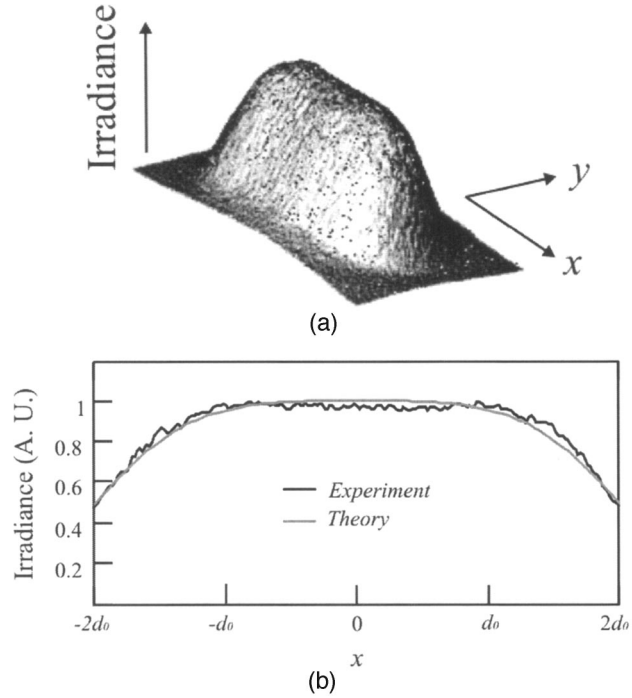

Fig. 9. Experimental irradiance distribution of a linear array of LEDs with $N = 4$. (a) The irradiance pattern when $m = 64.66$ and $d = d_0$. (b) Resulting normalized irradiance distribution along the x direction at $y = 0$.

4. Experimental Example

For the purpose of demonstration, we assembled a linear array of four LEDs with a LED-to-LED spacing of 1.84 cm. These LEDs (Steren 5/ULTRA WHITE) emit white light with a ranging angle of 30° and an angle $\theta_{1/2} = 8.44°$ ($m = 64.66$). From Eq. (13), the optimum LED-to-LED distance is $d_0 = 0.189z$. A translucent diffuse screen was positioned 9.74 cm from the LED array (optimum panel–target distance is $z = 9.74$ cm, which is measured from the chip image position, coinciding in our LEDs with the encapsulant base.) The light transmitted through the screen was imaged at a charge-coupled device (CCD) camera. The recorded irradiance pattern is shown in Fig. 9(a). Figure 9(b) shows the experimental and simulated irradiance distribution along the center axis of the array (horizontal direction). The slight disagreement between experimental and modeled data is explained by the fact that the irradiance patterns of assembled LEDs are not equal even among LEDs of the same type.[16] Nevertheless, the agreement between theoretical predictions and experimental data confirms that the derived expressions are practical design tools for both a quick estimation (first-order design) and the starting point for exact designs.

5. Conclusions

We have analyzed the optimum LED-to-LED spacing, i.e., the optimum packing density of light sources consisting of multiple LEDs to uniformly illuminate

near targets by considering each single LED as an imperfect Lambertian emitter.

Practical equations and formulas were derived for the optimum LED-to-LED spacing of six basic array configurations to achieve uniform near-field irradiance. These design tools offer an easy way to estimate the performance of LED arrays due to the parameters of the LEDs that assemble the array. The explicit dependence on optical parameter $\theta_{1/2}$ (typically provided by the manufacturer), the configuration geometry, and the number of LEDs that assemble the array make this analysis a practical tool for both a quick estimation (first-order design) and the starting point for an exact design. In particular, this analysis can be useful to begin exact designs of LED arrays that require time-consuming optical models of LED sources, e.g., measurement-based models and numerical models.[17,18] Recently we successfully applied the results of this research to design and assemble multicolor LED clusters for uniform color illumination.[19]

Using the derived optimum LED-to-LED spacing, irradiance patterns were displayed graphically for a two-LED array, a ring of LEDs, a ring with one middle LED, a linear array of LEDs, a square array of LEDs, and a triangular array of LEDs. An experiment with a linear array was performed to confirm our analysis. Experimental data agreed with theoretical expectations.

This research was supported by CONACYT (Consejo Nacional de Ciencia y Tecnologia) grant J48199-F.

References

1. Y. Narukawa, "White-light LEDs," Opt. Photon. News **15,** 24–29 (2004).
2. J. Wafer, "LEDs continue to advance," Photonics Spectra **39,** 60–62 (2005).
3. I. Moreno and R. I. Tzonchev, "Effects on illumination uniformity due to dilution on arrays of LEDs," in *Nonimaging Optics and Efficient Illumination Systems,* R. Winston, R. J. Koshel, eds., Proc. SPIE **5529,** 268–275 (2004).
4. T. Ito and K. Okano, "Color electroholography by three colored reference lights simultaneously incident upon one hologram panel," Opt. Express **12,** 4320–4325 (2004).
5. H. Yamamoto, M. Kouno, S. Muguruma, Y. Hayasaki, Y. Nagai, Y. Shimizu, and N. Nishida, "Enlargement of viewing area of stereoscopic full-color LED display by use of a parallax barrier," Appl. Opt. **41,** 6907–6919 (2002).
6. A. L. Dubovikov, S. S. Repin, and S. N. Natarovskii, "Features of the use of LEDs in artificial-vision systems," J. Opt Technol. **72,** 40–42 (2005).
7. L. Domjan, L. Kocsanyi, P. Richter, S. Varkonyi, and W. Feiten, "Stripe illuminator based on LED array and parabolic mirror for active triangulation sensors used on mobile robots," Opt. Eng. **39,** 2867–2875 (2000).
8. L. Repetto, E. Piano, and C. Pontiggia, "Lensless digital holographic microscope with light-emitting diode illumination," Opt. Lett. **29,** 1132–1134 (2004).
9. C. Deller, G. Smith, and J. Franklin, "Colour mixing LEDs with short microsphere doped acrylic rods," Opt. Express **12,** 3327–3333 (2004).
10. J. F. Van Derlofske and T. A. Hough, "Analytical model of flux propagation in light-pipe systems," Opt. Eng. **43,** 1503–1510 (2004).
11. F. Causa and J. Sarma, "Realistic model for the output beam profile of stripe and tapered superluminescent light-emitting diodes," Appl. Opt. **42,** 4341–4348 (2003).
12. D. Wood, *Optoelectronic Semiconductor Devices* (Prentice-Hall International, 1994), pp. 84–88.
13. G. O. Reynolds, J. B. DeVelis, G. B. Parrent, Jr., and B. J. Thompson, *The New Physical Optics Notebook* (SPIE Press, 1989), pp. 38–45.
14. C. J. Whitters, J. M. Girkin, and J. J. Carey, "Curing of dental composites by use of InGaN light-emitting diodes," Opt. Lett. **24,** 67–68 (1999).
15. Y. Kawakami, J. Shimada, and S. Fujita, "Fabrication of LED lighting goggle for surgical operation and approach toward high color rendering performance," in *Solid State Lighting and Displays,* I. T. Ferguson, Y. S. Park, N. Narendran, and S. P. DenBaars, eds., Proc. SPIE **4445,** 156–164 (2001).
16. J. M. Benavides and R. H. Webb, "Optical characterization of ultrabright LEDs," Appl. Opt. **44,** 4000–4003 (2005).
17. W. J. Cassarly, "LED modelling: pros and cons of common methods," Photon. Tech Briefs, pp IIa–2a (April 2002), special supplement to NASA Tech Briefs.
18. F. Hu, K. Y. Qian, and Y. Luo, "Far-field pattern simulation of flip-chip bonded power light-emitting diodes by a Monte Carlo photon-tracing method," Appl. Opt. **44,** 2768–2771 (2005).
19. I. Moreno and L. M. Molinar, "Color uniformity of the light distribution from several cluster configurations of multicolor LEDs," in *Fifth International Conference on Solid State Lighting,* I. T. Ferguson, J. C. Carrano, T. Taguchi, I. E. Ashdown, eds., Proc. SPIE **5941,** 359–365 (2005).